ESC European Society of Cardiology

European Heart Journal - Cardiovascular Imaging (2024) **25**, 188–198
https://doi.org/10.1093/ehjci/jead261

ORIGINAL PAPER

Post-Ablation cardiac Magnetic resonance to assess Ventricular Tachycardia recurrence (PAM-VT study)

Ivo Roca-Luque [1,2,3]*, Sara Vázquez-Calvo[1,2], Paz Garre[1,2], Jose T. Ortiz-Perez[1,2], Susanna Prat-Gonzalez[1,2], Paula Sanchez-Somonte[1,2], Elisenda Ferro[1,2], Levio Quinto[1,2], Francisco Alarcón[1,2,3], Till Althoff[1,2], Rosario Jesús Perea[2,4], Rosa M. Figueras i Ventura[5], Eduard Guasch [1,2,3], José Maria Tolosana[1,2,3], Daniel Lorenzatti[1,2], Carlos Igor Morr-Verenzuela[1,2], Andreu Porta-Sanchez [1,2,3], Elena Arbelo[1,2,3], Marta Sitges [1,2,3], Josep Brugada [1,2,3], and Lluís Mont [1,2,3]

[1]Arrhyhtmia Section, Institut Clínic Cardiovascular, Hospital Clínic, Universitat de Barcelona, Villarroel st. 170, Catalonia, 08036 Barcelona, Spain; [2]Institut d'Investigacions Biomèdiques August Pi i Sunyer (IDIBAPS), Barcelona, Catalonia, Spain; [3]Centro de Investigación Biomédica en Red de Enfermedades Cardiovasculares (CIBERCV), Madrid, Spain; [4]Centre de Diagnòstic per la Imatge, Hospital Clínic, Universitat de Barcelona, Catalonia, Spain; and [5]Adas3D Medical S.L., Barcelona, Spain

Received 12 May 2023; revised 4 September 2023; accepted 24 September 2023; online publish-ahead-of-print 11 October 2023

See the editorial comment for this article 'Post-ablation cardiac magnetic resonance in ventricular tachycardia ablation: shining light on dark cores and corridors', by P. Bhagirath, https://doi.org/10.1093/ehjci/jead275.

Aims Conducting channels (CCs) detected by late gadolinium enhancement cardiac magnetic resonance (LGE-CMR) are related to ventricular tachycardia (VT). The aim of this work was to study the ability of post-ablation LGE-CMR to evaluate ablation lesions.

Methods and results This is a prospective study of consecutive patients referred for a scar-related VT ablation. LGE-CMR was performed 6–12 months prior to ablation and 3–6 months after ablation. Scar characteristics of pre- and post-ablation LGE-CMR were compared. During the study period (March 2019–April 2021), 61 consecutive patients underwent scar-related VT ablation after LGE-CMR. Overall, 12 patients were excluded (4 had poor-quality LGE-CMR, 2 died before post-ablation LGE-CMR, and 6 underwent post-ablation LGE-CMR 12 months after ablation). Finally, 49 patients (age: 65.5 ± 9.8 years, 97.9% male, left ventricular ejection fraction: 34.8 ± 10.4%, 87.7% ischaemic cardiomyopathy) were included. Post-ablation LGE-CMR showed a decrease in the number (3.34 ± 1.03 vs. 1.6 ± 0.2; $P < 0.0001$) and mass (8.45 ± 1.3 vs. 3.5 ± 0.6 g; $P < 0.001$) of CCs. Arrhythmogenic CCs disappeared in 74.4% of patients. Dark core was detected in 75.5% of patients, and its presence was not related to CC reduction (52.2 ± 7.4% vs. 40.8 ± 10.6%, $P = 0.57$). VT recurrence after one year follow-up was 16.3%. The presence of two or more channels in the post-ablation LGE-CMR was a predictor of VT recurrence (31.82% vs. 0%, $P = 0.0038$) with a sensibility of 100% and specificity of 61% (area under the curve 0.82). In the same line, a reduction of CCs < 55% had sensibility of 100% and specificity of 61% (area under the curve 0.83) to predict VT recurrence.

Conclusion Post-ablation LGE-CMR is feasible, and a reduction in the number of CCs is related with lower risk of VT recurrence. The dark core was not present in all patients. A decrease in VT substrate was also observed in patients without a dark core area in the post-ablation LGE-CMR.

* Corresponding author. E-mail: iroca@clinic.cat

Graphical Abstract

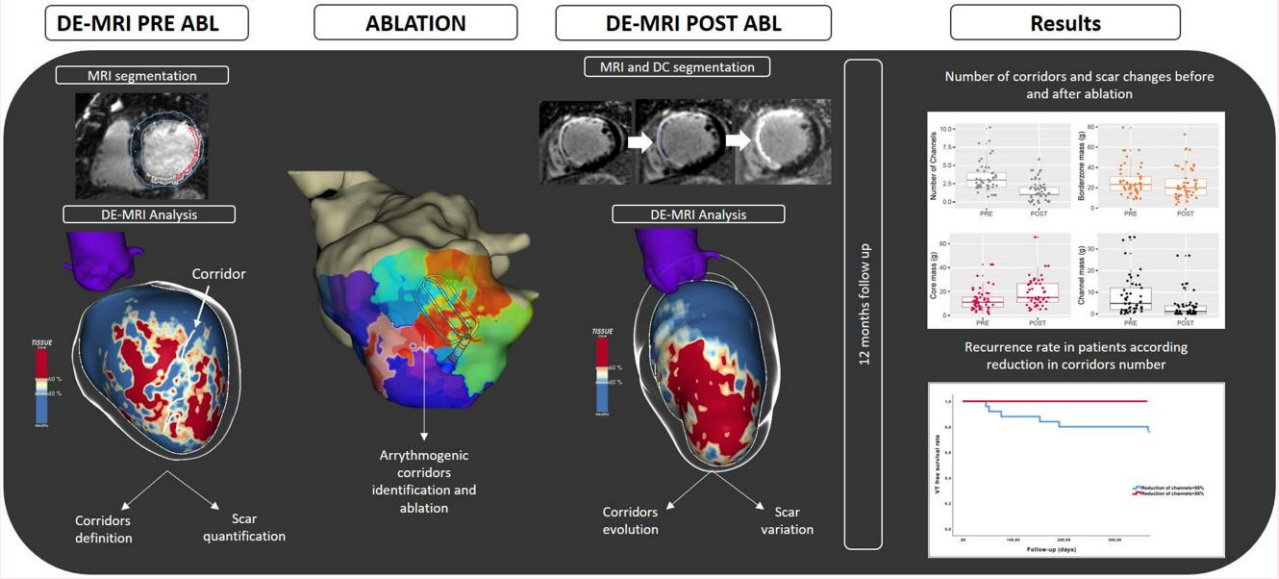

Keywords ventricular tachycardia • ventricular tachycardia ablation • cardiac magnetic resonance • scar characterization • late gadolinium enhancement

Introduction

Substrate-based radiofrequency catheter ablation has become a standard procedure for the treatment of scar-related ventricular tachycardia (VT). The main mechanism behind scar-related VT is the presence of a re-entrant circuit. This circuit is formed by the presence of a slow conduction area within the scar that connects to the healthy non-scarred myocardium, leading to re-entry. These regions are also called conducting channels (CCs) and can be accurately identified with electroanatomical maps (EAMs) during ablation.[1,2]

Likewise, late gadolinium enhancement cardiac magnetic resonance (LGE-CMR) has been demonstrated to be able to identify and characterize this arrhythmogenic substrate with unprecedented precision, being able to depict CCs[3–5] and deceleration zones (DZs).[6] Pre-procedural LGE-CMR is gaining widespread applicability as an assistance tool in ablation procedures since it can facilitate procedural planning, scar mapping and ablation,[7,8] and for the evaluation of the risk of recurrences after ablation.[9] However, the majority of patients scheduled for VT ablation has an implantable cardioverter defibrillator (ICD).[10] This issue represents a major limitation affecting image quality with conventional LGE-CMR. The use of wideband (WB) sequences can overcome this limitation by minimizing device-related artefacts, making LGE-CMR imaging robust for myocardial characterization under these conditions.[11–13] In this sense, a good correlation between WB LGE-CMR and EAM has recently been demonstrated in previous work from our group.[6,14]

Despite the use of pre-procedural LGE-CMR to aid VT ablation, clinical data on whether LGE-CMR is capable of identifying ablation lesions and its relation to VT recurrence are still lacking. A few studies, including some with pathological correlations, have reported LGE-CMR findings following catheter ablation. Based on animal models,[15,16] the appearance of ablation lesions is different in the acute phase than in the chronic phase. In the acute phase, due to haemorrhage, coagulative necrosis, and subsequent microvascular obstruction (MVO), the appearance is a dark area on post-contrast T1-weighted imaging (so-called 'dark core') surrounded by a peripheral rim of enhancement. In the chronic phase, as gadolinium contrast fills in, the ablation lesions are depicted as fully bright areas by LGE-CMR imaging, resembling the scar seen in chronic infarct patients. However, a recent retrospective observational study[17] suggests that the typical appearance in the acute state can persist during chronic follow-up, particularly when ablation lesions are produced on top of scarred tissue. That study included only patients who underwent repeated ablations for whom post-ablation LGE-CMR was not initially planned, and consequently, the elapsed time from ablation to LGE-CMR was very heterogeneous. Interestingly, dark core areas observed in post-ablation LGE-CMR were related with the ablated areas (correlation of 79 ± 15%) and more important, dark core areas were proved to be non-excitable tissue in the redo procedures (R 0.98, $P < 0.01$, Dice Score 0.84). To our knowledge, no prospective study addressing the role of post-ablation LGE-CMR in evaluating ablation results has been published. The aim of this prospective study with pre-specified control post-ablation LGE-CMR is to analyse the usefulness of this imaging test for evaluating ablation results and quantifying changes in the arrhythmogenic VT substrate.

Methods

Study population

This is a prospective observational study of all consecutive patients who underwent the first procedure of substrate-based VT ablation at a single centre (Hospital Clinic) between March 2019 and July 2020. All patients underwent LGE-CMR within the 6–12 months before and 3–6 months after the ablation procedure. Patients without LGE-CMR or those with suboptimal image quality were excluded. Patients with ventricular arrhythmias caused by reversible causes or focal VT ablation and/or without scarring on pre-procedural LGE-CMR were also excluded. All patients provided written informed consent. The study was carried out according to the Declaration of Helsinki guidelines and the deontological code of our institution. The study protocol was approved by the ethical committee of the hospital.

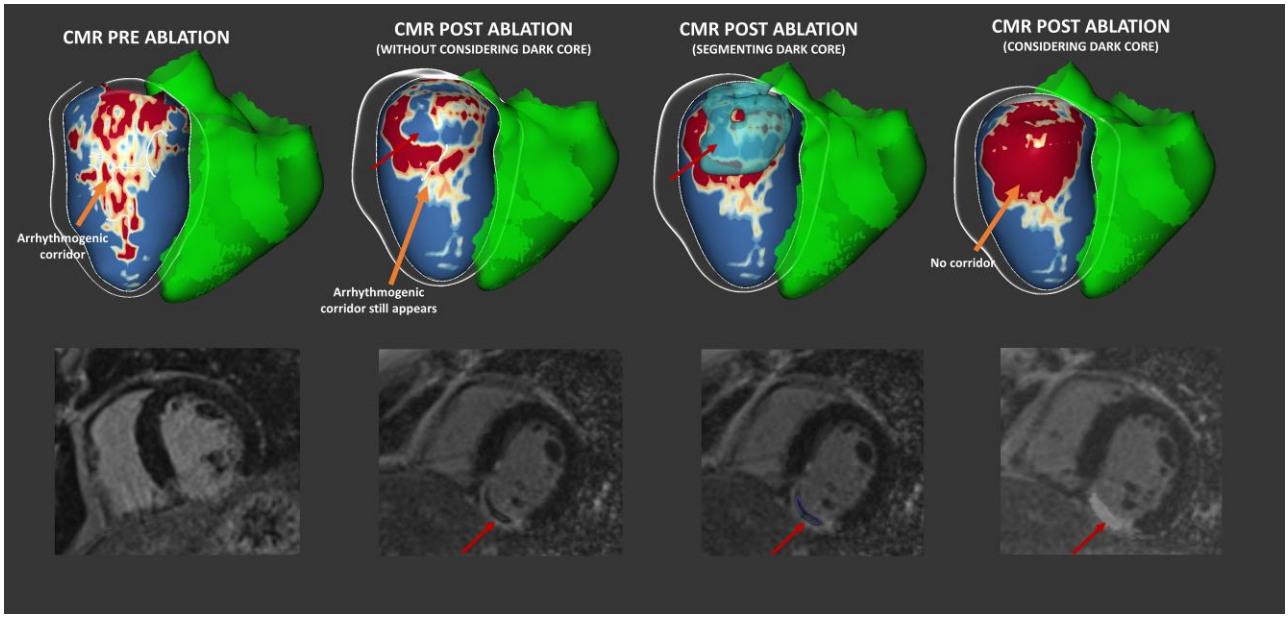

Figure 1 Cardiac magnetic resonance segmentation integrating dark core. In the bottom panels, the raw images of LGE-CMR are shown. In the upper panels, the same images in posteroanterior view after post-processing by ADAS3D are visualized. In the first panel, pre-ablation LGE-CMR reveals an arrhythmogenic channel inside the scar. In the second panel, the LGE-CMR post-ablation segmentation is shown without considering the DC (red arrow) as dense fibrosis. In this case, the software will code that area as healthy tissue because of the hypointense pixel intensity, showing the persistence of the arrhythmogenic channel and therefore, considering the ablation procedure incomplete. In the third and fourth panels, the same post-ablation LGE-CMR is shown, but the DC area has been manually delineated (light blue area, red arrow). The maximum pixel intensity threshold used to define the scar core was selected to convert the manually selected hypointense DC area into hyperenhancement scar core. Last panel shows the final LGE-CMR reconstruction, where the pre-ablation arrhythmogenic channel does not appear, so ablation can now be considered successful in terms of arrhythmogenic channel abolition.

Procedural data

Procedures were performed under general anaesthesia. After femoral venous access, a multipolar diagnostic catheter was positioned at the right ventricular (RV) apex. According to the arrhythmogenic substrate detected by LGE-CMR and VT ECG (if available), EAMs of the left ventricle (LV) and RV were obtained during RV-paced rhythm using an Ensite Precision (Abbott Medical, USA) navigation system. EAMs were created with a high-definition grid mapping catheter (Advisor HD Grid, Abbott Medical, USA). Bipolar voltage mapping was performed using established voltage settings of <0.5 mV for dense scarring and <1.5 mV for border zone (BZ).[18] Automated annotation was performed at the offset of the latest local electrogram (EGM) component using Last Deflection (Abbott Medical, USA) algorithm. Late potentials, fragmented potentials, DZs[19], and any abnormal EGM were also manually tagged during mapping to define CCs inside the scar.

After substrate mapping during paced rhythm, VT was induced by programmed electrical stimulation (drive cycles of 600 and 400 ms, up to three extrastimuli to refractoriness or 200 ms). When VT was haemodynamically tolerated, detailed activation mapping for diastolic and presystolic activity was performed. In cases in which VT was not haemodynamically tolerated, the VT isthmus was defined as the area with a fast transition of good pace mapping (suggesting the VT exit site) and poor pace mapping (suggesting the VT entrance site), as described previously by Chillou.[20] Radiofrequency was delivered using an externally irrigated 3.5 mm tip contact force sensor ablation catheter (Tacticath SE, Abbott Medical, USA) with 45°C temperature control, 40–50 W power limit, and 26–30 mL/min irrigation rate. The ablation endpoint was both non-inducibility and abolishment of late potentials, local abnormal ventricular activities, and DZs confirmed with a complete remap.

Data from LGE-CMR

LGE-CMR was performed using either a 1.5 Tesla (Magnetom Aera, Siemens Healthcare, Germany) or 3 Tesla scanner (Magnetom Trio, Siemens Healthcare, Germany) in participants with or without an ICD, respectively. For those with an ICD, a WB sequence was applied to abolish device-related artefacts.[14]

Technical details about LGE-CMR protocol are previously described by our group: wideband sequence in ICD patients[14] and 3D sequence in patients without ICD.[4]

Patients with ICD (wideband sequence)

First of all, in order to reduce possible damage to the ICD and the surrounding tissue by temperature and possible changes in thresholds and impedances, the specific absorption rate was limited to <2 W/kg. Specific workflow was performed before CMR in patients with an ICD; a trained electrophysiologist interrogated ICD parameters and all therapies and detections were disabled. Blood pressure, pulseoximetry, and heart rate were monitored during CMR. After several standard scout slices, an intravenous bolus of 0.2 mmol/kg of gadobutrol (Gadovist, BayerHispaniaSL) was injected. Seven to 10 min after the injection, WB LGE-CMR images were obtained using a WB inversion pulse sequence (3.8 kHz) in serial short-axis slices (5 mm slice thickness, no gap) covering the whole LV from the base to the apex. The inversion time was adjusted to null normal myocardium (increasing between 200 and 320 ms typically).

Patients without ICD (3D sequence)

A whole-heart, high spatial resolution, delayed-enhanced study was conducted using a commercially available free-breathing, 3D-GRE

inversion-recovery gradient echo technique (gradient echo read out). The 3D slab was acquired in the axial plane. A Cartesian trajectory was used to fill the k-space with phase-encoding (y) in the anteroposterior direction. The field of view was covered by a 256 × 240 pixel matrix, and in-plane reconstruction was allowed to achieve an isotropic spatial resolution of 1.4 × 1.4 × 1.4 mm and a voxel size of 2.74 mm^3. To compensate for the long acquisition time anticipated, we added 50 ms to the nominal value necessary to null normal myocardium, as derived from the TI scout. Other typical sequence parameters were as follows: repetition time 440 ms; echo time 1.29 ms; flip angle 158; band width 810 Hz/pixel; and 51k-space lines filled per heartbeat. In some cases, a high temporal resolution, four-chamber view cine, achieved by means of parallel imaging with an acceleration factor of 3, was used to select the optimal acquisition window and minimize cardiac motion in late-diastole. Respiratory synchronization was performed for every other heartbeat using a crossed-pair navigator approach. The data set was acquired during expiration and generalized, autocalibrating, partially parallel acquisition with an acceleration factor of 2 was used to speedup data acquisition. A set of images was reconstructed in the left ventricle (LV) short-axis orientation with 1.4 mm slice thickness (typically 50–70 images) for subsequent image processing. A new TI scout was prescribed to select an updated TI.

All LGE-CMR images were processed using a previously described protocol reported briefly here.[4,21] Full LV volume was reconstructed in the short-axis orientation, and the resulting images were processed with ADAS3D software (ADAS 3D, Barcelona, Spain). After semi-automatic delineation of the endocardium and epicardium, nine concentric equally spaced surface layers were created. A 3D shell was obtained for each layer. PSI (pixel signal intensity) maps were obtained from LGE-CMR images, projected to each of the shells following a trilinear interpolation algorithm and colour coded (core scar in red, BZ in yellow, and healthy tissue in blue). A PSI-based algorithm was applied to characterize the hyperenhanced areas using 40 ± 5% (healthy tissue) and 60 ± 5% (core scar) of the maximum intensity signal as thresholds. A CC on the LGE-CMR reconstruction was defined as a channel of BZ between two core areas, whether observed in the same layer or between consecutive layers. Depending on the LGE distribution from 10% (the layer closest to the endocardium) to 90% (the layer closest to the epicardium), the substrate was defined as subendocardial when LGE affected 10% to 30% of the layer, epicardial when LGE affected 60% of the outer layer and midmyocardial when LGE was confined to the internal layer of myocardial thickness (layer 40–60%). Areas of LGE > 75% in the myocardial thickness were considered transmural. Septal involvement was considered when more than 40% of the septal thickness presented LGE distribution in any portion. The arrhythmogenic channel was defined as the CMR channel correlated with the VT isthmus during the procedure.

Dark core definition and post-procedural LGE-CMR analysis

Because dark core (DC) lesions observed in conventional LGE imaging acquired 10 to 15 min after contrast administration appear black in post-contrast T1-weighted imaging, they can therefore be misinterpreted as healthy or BZ tissue during the segmentation process. Indeed, CCs could be incorrectly annotated if the DC area is inside the core scar. Therefore, in this study, it was considered essential to identify the presence of catheter-induced DC lesions by performing a side-by-side comparison of the pre- and post-ablation LGE-CMR studies. The coregistered short-axis slices from the pre- and post-ablation LGE studies were simultaneously presented to observers (blinded to EAM data) experienced in LGE-CMR interpretation who manually and roughly delineated DC areas. The defined criteria for DC areas was the presence, in the post-ablation LGE-CMR, of a hypointense region with signal intensity below the mean signal intensity of the non-enhanced myocardium, and surrounded by hyperenhanced myocardium not observed in the pre-ablation LGE-CMR study. Next, the maximum pixel intensity threshold used to define the scar core was selected to convert the manually selected hypointense DC areas into scar core. Therefore, those areas

Table 1 Population and procedural characteristics

Clinical characteristics	Patients studied ($n = 49$)
Age (years)	65.5 ± 9.8 (24–78)
Male sex	48 (98.0%)
Hypertension	40 (81.6%)
Diabetes	25 (51%)
Dyslipidaemia	37 (75.5%)
COPD	6 (12.2%)
CKD	13 (26.5%)
NYHA class	I–II: 33 (67.3%)
	III–IV: 13 (32.7%)
Ischaemic cardiomyopathy	43 (87.7%)
Permanent AF	6 (12.2%)
Sotalol therapy	4 (8.1%)
Amiodarone therapy	32 (65.3%)
Mexiletine therapy	3 (6.1%)
Previous ICD	42 (85.7%)
VT storm	7 (14.2%)
Incessant VT	3 (6.1%)
LVEF (%)	34.8 ± 10.5 (15–60)
LVEDD (mm)	61.4 ± 7.9 (40–75)
CMR characteristics	
Scar location	
Anterior/anterolateral	17 (34.7%)
Septal	13 (26.5%)
Inferior	19 (38.8%)
Scar transmurality	
<25%	12 (24.4%)
25–50%	20 (41.4%)
50–75%	7 (14.7%)
>75%	10 (20.4%)
Procedural characteristics	
Contact force catheter	40 (83.6%)
Transeptal access	44 (89.8%)
Epicardial access	6 (12.2%)
Number of EAM points	1358.3 ± 1103.1
Number of VT inductions	1.81 ± 1.6 (0–9)
Number of VT mapped	1.32 ± 1.6 (0–9)
Number of RF applications	58 ± 20.9 (9–99)
RF time (seconds)	1896 ± 789.4 (399–3000)
Procedural time (minutes)	228.1 ± 73.8
Final non-inducibility	44 (89.8%)
Residual slow conduction	7 (14.8%)

ICM, ischaemic cardiomyopathy; COPD, chronic obstructive pulmonary disease; CKD, chronic kidney disease; AF, atrial fibrillation; VT, ventricular tachycardia; ICD, implantable cardioverter defibrillator; NYHA, New York Heart Association; LVEDD, left ventricle end-diastolic diameter; LVEF, left ventricular ejection fraction.

Table 2 Post-ablation LGE-CMR characteristics

	Pre	Post	P
Number of channels detected	3.34 ± 1.03	1.61 ± 0.4	<0.0001
Channels (grams)	8.45 ± 1.3	3.5 ± 0.6	<0.0001
LV mass (grams)	165 (IQR 132 199)	155 (IQR 127 198)	0.87
Core (grams)	13.2 ± 9.21	19.3 ± 11.8	<0.0001
BZ (grams)	26.5 ± 14.8	23.7 ± 14.9	0.26
Scar heterogenicity (BZ area/total scar area)	69.1 ± 9.3%	54.7 ± 13.6%	0.002

LV, left ventricular; BZ, border zone.

Table 3 Relation of dark core with LGE-CMR and ablation parameters

	Presence of dark core (37)	Absence of dark core (12)	P-value
Time to ablation post-procedural LGE-CMR (days)	152.2 ± 52.3	138.1 ± 35.7	0.74
RF time (seconds)	2128.9 ± 130.6	1567.2 ± 245.3	0.06
Reduction in CCs (%)	52.2 ± 7.4%	40.8 ± 10.6	0.57
Reduction in CC mass (%)	59.1 ± 10.7%	36.6 ± 28.3	0.16
VT recurrence rate	16.2%	16.7%	0.91

LGE-CMR, late gadolinium enhancement cardiac magnetic resonance; RF, radiofrequency; CC, conducting channel; VT, ventricular tachycardia.

will appear in white in the new PSI map and coded as dense fibrosis (*Figure 1*).

Follow-up data

Patients were followed up at 3, 6, and 12 months and then yearly after ablation, and their ICDs were monitored for episodes of ventricular arrhythmia. During follow-up, a reduction or discontinuation of antiarrhythmic drugs was considered at the clinician's discretion. VT recurrence was defined as any VT episode longer than 30 s or episode that required ICD intervention. All sustained VT events, ICD therapies, and new hospitalizations were recorded.

Statistical analysis

Continuous data are reported as the means ± SDs or median and interquartile range (IQR) in case of variables without a normal distribution, and comparisons between groups were performed using Student's *t*-test or the Mann–Whitney *U* test, as appropriate. Categorical variables are expressed as the total number and percentage and were compared between groups using the χ^2 or Fisher's test or two-way ANOVA for non-dichotomous categorical variables. Receiver operating characteristic curves were calculated to estimate the predictive value of scar variables and to identify cut-off points. All analyses were performed with SPSS v18.0 (SPSS, Chicago, IL, USA) and R software for Windows version 3.6.1 (R project for Statistical Computing; Vienna, Austria). All statistical tests were two-sided, and a *P*-value < 0.05 was considered statistically significant.

Results

Study population

A total of 72 patients with structural heart disease underwent a first procedure scar-related VT ablation at a single centre from March 2019 to December 2020. In 11 patients, pre-procedural LGE-CMR was not performed because of formal contraindication (8 patients) or because they refused to LGE-CMR (3 patients). Of the 61 patients who underwent pre-procedural LGE-CMR, 4 patients had poor-quality LGE-CMR; 2 patients died before post-procedural LGE-CMR, and 6 patients underwent LGE-CMR after the designed period. Overall, the final population consisted of 49 patients (age: 65.5 ± 9.8 years; male, 98%). The most frequent underlying disease was ischaemic heart disease (87.7%). The basal characteristics of the study population (including LGE-CMR data) are shown in *Table 1*. Regarding LGE-CMR, no differences were observed in ischaemic cardiomyopathy (ICM) vs. non-ischemic cardiomyopathy (NICM) patients: BZ mass median 21 g, (IQR 17.4–32.4) vs. 25.2 (IQR 20.6–32.7) in NICM patients ($P = 0.75$), channel mass: median 5 (IQR 2.2–11.5) vs. 2.4 (IQR 1.0–8.5) ($P = 0.09$) and core mass: median 11 (IQR 7.1–18.1) in ICM vs. 7.7 (IQR 5–10.1) in NICM patients ($P = 0.16$).

Procedural data

VT ablation was performed with an exclusively endocardial approach in 44 (89.8%) patients and an endoepicardial approach in 5 patients. Major complications occurred in 4.1% (2) of the patients. VT could be induced in 34 (82.9%) patients, and an isthmus could be defined in 41 (83.6%) of these patients. Non-inducibility and complete abolition of late potentials were achieved in 44 (89.8%) and 42 (85.2%) patients. The characteristics of the procedure are summarized in *Table 1*.

LGE-CMR substrate characterization

Table 2 describes pre- and post-procedural substrate LGE-CMR-derived data. Regarding CCs, before the procedure, the mass and number of channels were 8.45 ± 1.32 g and 3.34 ± 0.32 channels, respectively.

Channels reduction after ablation

After the procedure, both mass and number of channels were reduced to 3.34 ± 1.03 g ($P < 0.001$) and 1.6 ± 0.2 channels ($P < 0.0001$), respectively. A reduction of more than 50% in CC mass was observed in 33 patients (67.3%). Accordingly, in 26 patients (53.1%), a reduction of more than 50% in the number of channels was achieved.

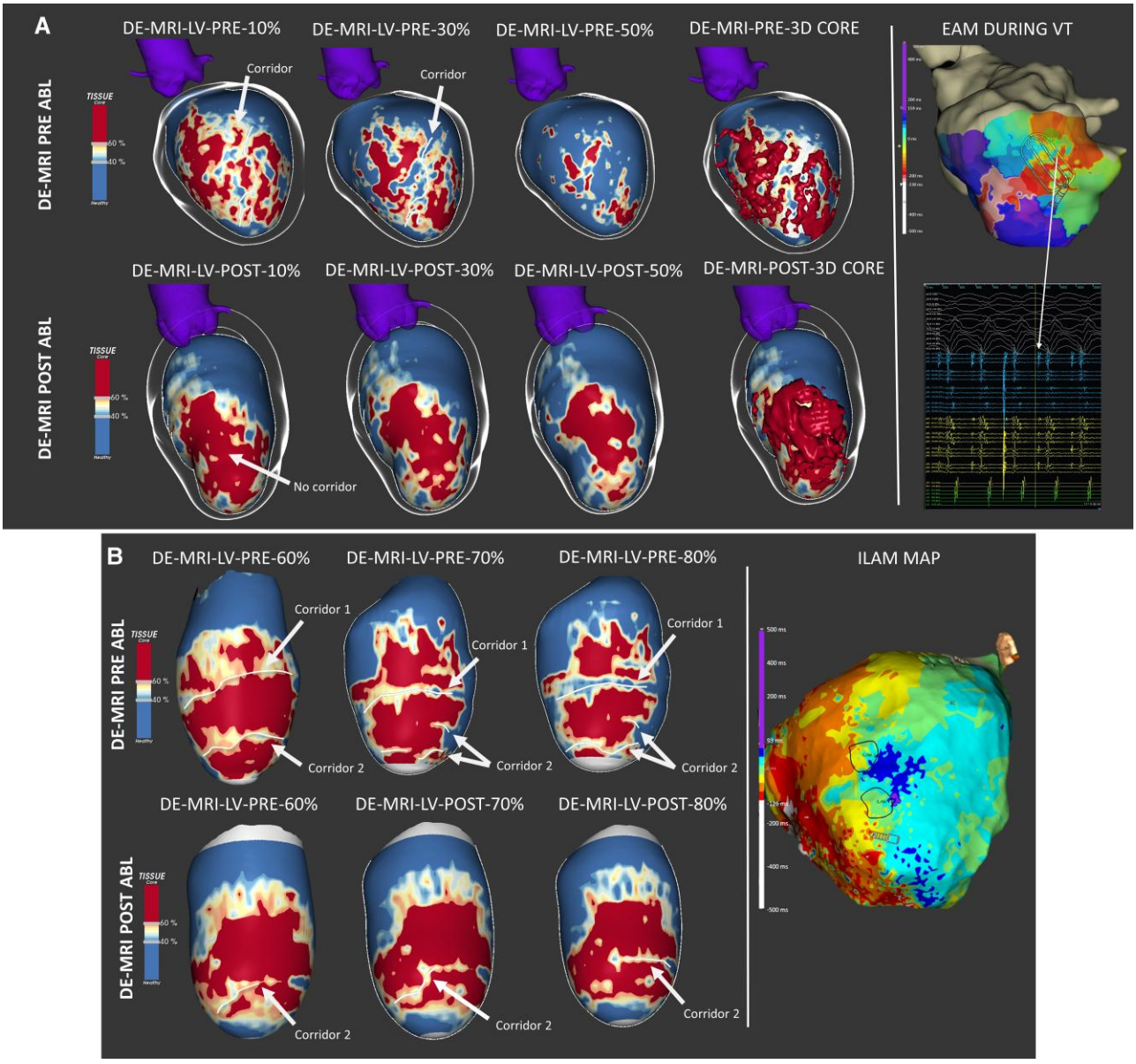

Figure 2 Arrhythmogenic channel visualization in the post-ablation LGE-CMR. Upper panel: three-dimensional reconstruction of pre-ablation LGE-CMR with the endocardial channel in the anterior wall (white arrow) from layer 10% to 30%. In the right panel activation map during VT with a clear figure-of-eight circuit using the channel shown in the LGE-CMR with diastolic potentials inside the channel. Bottom panel: three-dimensional reconstruction of LGE-CMR of the same patient 3 months after the ablation procedure. There is an increase in dense scarring produced by radiofrequency ablation that leads to the disappearance of the arrhythmogenic endocardial channel. After one year of follow-up, the patient was free of VT recurrence. Upper panel: left anterior oblique view of three-dimensional reconstruction of pre-ablation LGE-CMR with two arrhythmogenic epicardial channels. In the right panel, an isochronal late activation map during sinus rhythm is shown revealing the presence of two deceleration zones (black circles) that correspond to the entrances of both channels. Bottom panel: three-dimensional reconstruction of LGE-CMR in the same patient 3 months after the ablation procedure. There is an increase in dense scarring, but channel 1 still appears. This patient recurred presenting three VT episodes within the first 6 months after ablation.

An arrhythmogenic channel in the pre-procedural LGE-CMR was identified in 43 patients (87.7%). In 29 of these patients (67.4%), the channel disappeared in the post-ablation LGE-CMR (*Figure 2*). In the rest of the patients, the arrhythmogenic channel was still visible in the post-ablation LGE-CMR with a smaller BZ mass (pre-ablation: 8.9 ± 2.5 vs. post-ablation: 6.3 ± 2.2; $P < 0.001$) and less transmurality (number of layers affected: pre-ablation 4.7 ± 0.8 vs. post-ablation 2.8 ± 0.61; $P = 0.04$) (*Figure 3*).

Core scar, BZ, and dark core

Regarding the remaining scar characteristics, after ablation, there was an increase in core scar (19.3 ± 11.8 vs. 13.2 ± 9.21 g; $P < 0.0001$)

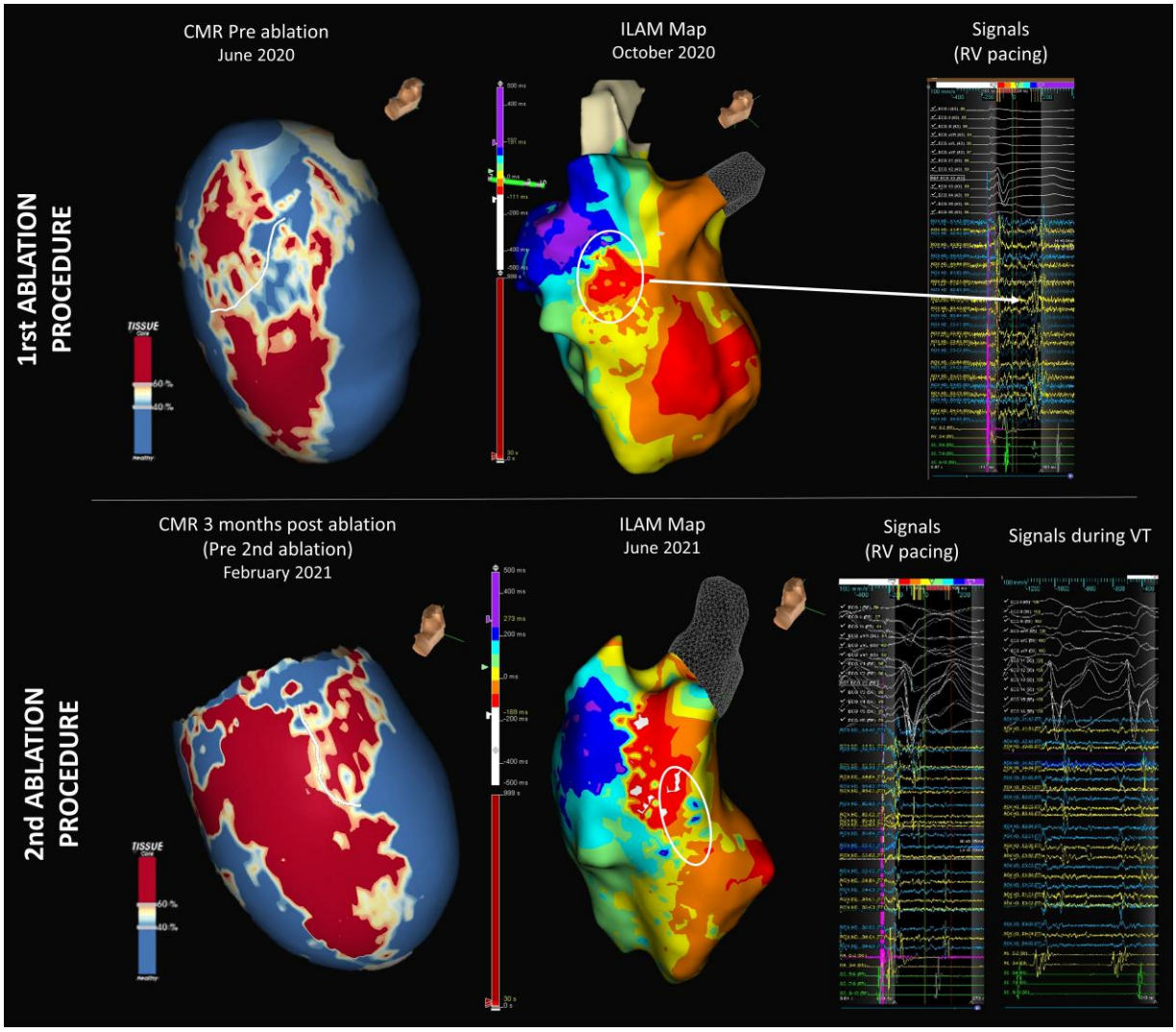

Figure 3 Channel visualization in a redo procedure. The upper panel shows LGE-CMR (before the first ablation procedure) with a clear CC in the posteroseptal scar in concordance with the DZ (white circle) in the isochronal late activation map (ILAM). Late and fragmented potentials were detected in that area (right panel). The bottom panel shows the 3-month post-ablation LGE-CMR with more homogenous scarring and disappearance of the more posterior part of the CC but a new exit in the anterior part of the scar (probably reconnection or incomplete ablation). The ILAM map shows the area of blockage in the upper part of the scar and a DZ in the new CC exit (with circle) with late potentials during RV pacing and diastolic potentials during VT.

without an increase in the area of BZ (26.5 ± ≡4.8 vs. 23.7 ± 14.9;P = 0.26). Indeed, there was a reduction in the heterogenicity of the scar in terms of the percentage of BZ over total scarring (post-ablation 54.7 ± 13.6% vs. 69.1 ± 9.3% before ablation; P = 0.002). Scar characteristics before and after ablation are shown in *Table 2* and *Figure 4*.

A 'dark core' area was detected in 37 patients (75.5%), but no association was found with the elapsed time between ablation and post-procedural LGE-CMR, RF time, reduction in the number of CCs, or CC mass and neither with VT recurrence rate (16.2% vs. 16.7%, P = 0.91). In *Table 3*, relation of DC with LGE-CMR and ablation parameters is shown.

Follow-up

After one year of follow-up, eight patients (16.2%) presented VT recurrence. Reduction of the number of CCs (49.0 ± 8.2% vs. 5 ± 3.2%; P = 0.02) was related with absence of VT recurrence. The presence of two or more channels in the post-ablation LGE-CMR was a predictor of VT recurrence (31.82% vs. 0%, P = 0.0038) with a sensibility of 100% and specificity of 61% (area under the curve 0.82). In the same line, a reduction of <55% of CCs predicts VT recurrence (28.57% vs. 0%, P < 0.0001, *Figure 5*) with a sensibility of 100% and specificity of 67% (area under the curve 0.83, *Figure 6*). No other post-ablation LGE-CMR -related parameter was related to VT recurrence (*Table 4*).

Discussion

Our study, to our knowledge, is the first to prospectively analyse the role of LGE-CMR in evaluating VT ablation results. The main finding is the strong relation of the degree of reduction of CCs with VT recurrence rate. A clear reduction in BZ and CCs is observed after ablation, thus resulting in an homogenization of the scar with and increased total dense scarring without an increase in the amount of BZ. These changes

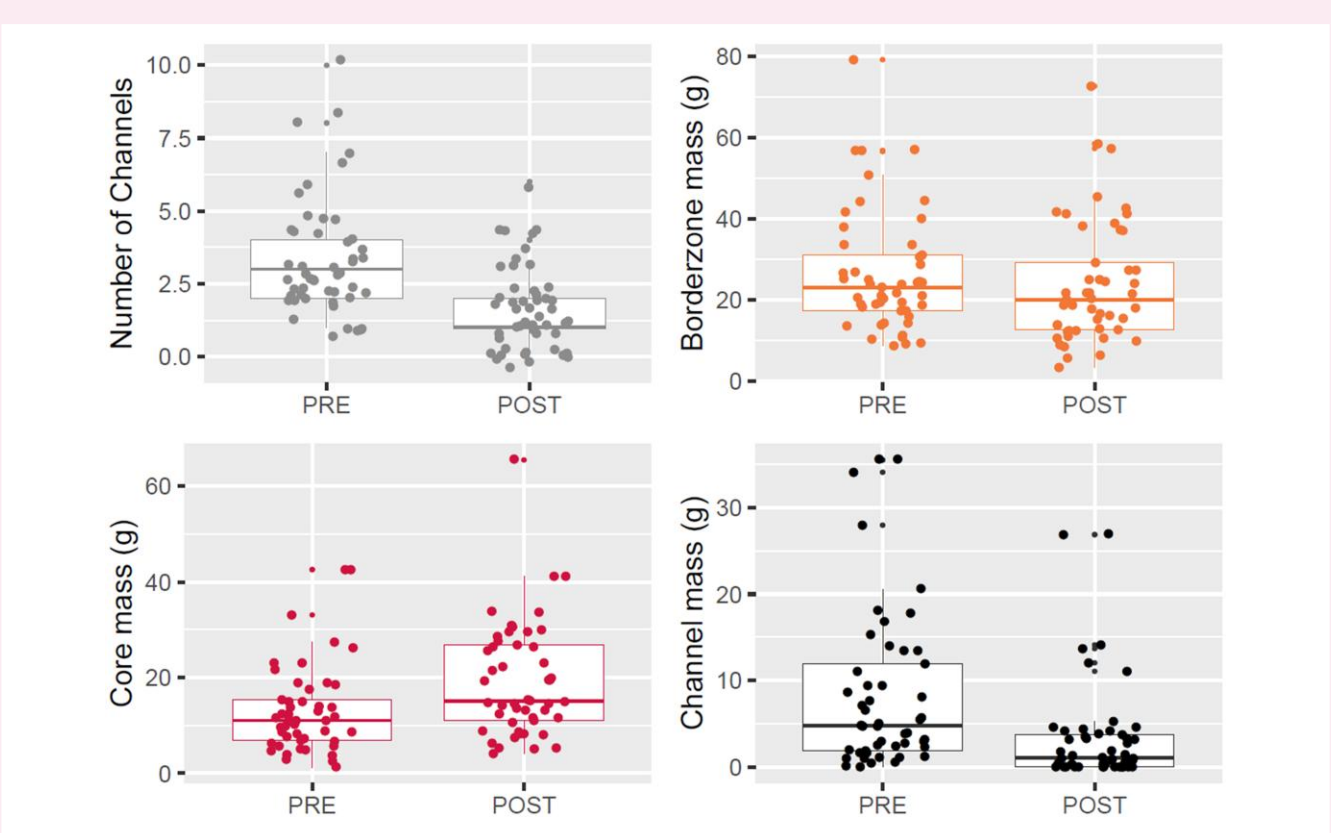

Figure 4 Scar characteristics before and after ablation. Comparison of LGE-CMR scar characteristics before and after ablation. A clear decrease in channel mass and number of channels is observed with an increase in core mass and no differences in BZ mass.

in scar can be detected by post-ablation LGE-CMR and are useful to stratify VT recurrence risk. Another important finding is the observations about the DC phenomenon in relation to MVO in the area of ablation lesions. DC has been historically related to ablation lesions and can be acutely visualized by LGE-CMR as DC even at the 3–6 months follow-up. However, in our study, its presence is neither constant nor clearly related to the percentage of CC mass reduction, so it is not a good marker of ablation lesion evaluation.

Reduction in CCs and scar changes

As stated before, CCs have been shown to be related to the VT isthmus and can be precisely detected by both EAMs and pre-procedural LGE-CMR.[1–5] The presence, extent, heterogenicity, and qualitative distribution of BZ tissue in myocardial scarring detected by LGE-CMR independently predict appropriate ICD therapies and sudden cardiac death.[22,23] In addition, CCs have also been proven to be related to appropriate therapies in patients with an ICD implanted for primary prevention.[22] In this sense, a reduction in CCs with post-procedural LGE-CMR can hypothetically be a non-invasive surrogate to evaluate the completeness of ablation. One of the main limitations of LGE-CMR in patients who have undergone VT ablation is that most of them have ICD *in situ*, so a major image artefact derived from an ICD device can minimize the post-procedural LGE-CMR quality. However, with the use of a dedicated LGE-CMR sequence (wideband sequence) to minimize ICD artefacts, LGE-CMR images have been highly improved. Indeed, the concordance of CCs in pre-ablation wideband LGE-CMR in patients with an ICD with CCs in the EAM has been proven to be as good as that in patients without ICD.[14] The use of imaging to evaluate ablation results has been shown to be useful in the field of atrial fibrillation ablation.[24] However, very little information has been published in the field of ventricular arrhythmias. In our prospective study, there was a significant reduction in the total amount of CCs and the CC mass. Changes in LGE-CMR after ablation were analysed in a small study[25]; however, the study population was different (one-third of patients did not have scarring before ablation), and there was no detailed analysis of scar characteristics, such as BZ mass, core scar mass, and CC details. Moreover, in that study, the post-ablation LGE-CMR findings were not related to ablation success. In our study, there was a reduction not only in CC number and mass but also in scar heterogenicity (percentage of BZ over total scar). In addition, we have proven that the degree of reduction of CCs was a predictor of VT recurrence after one year follow-up. Therefore, a reduction in CCs and scar heterogenicity in the post-ablation LGE-CMR could be a marker of ablation success and can lead to a tailored management of the patients after ablation.

Dark core to identify ablation lesion

The use of LGE-CMR to evaluate RF ablation lesions has been studied in the acute phase (4–8 weeks)[26] showing an area of no enhancement due to MVO also called the 'dark core' in post-contrast T1-weighted imaging. In a recent paper, these DC areas were related to the area of the ablation lesion[16] and were observed in all patients. This work included 17 non-consecutive patients who underwent post-ablation LGE-CMR before a redo VT ablation procedure. Only 10 of these patients had pre-procedural LGE-CMR. Although the delay between the index ablation procedure and the LGE-CMR study was 30 ± 29 months, a 'dark core' was observed in all patients and was related to

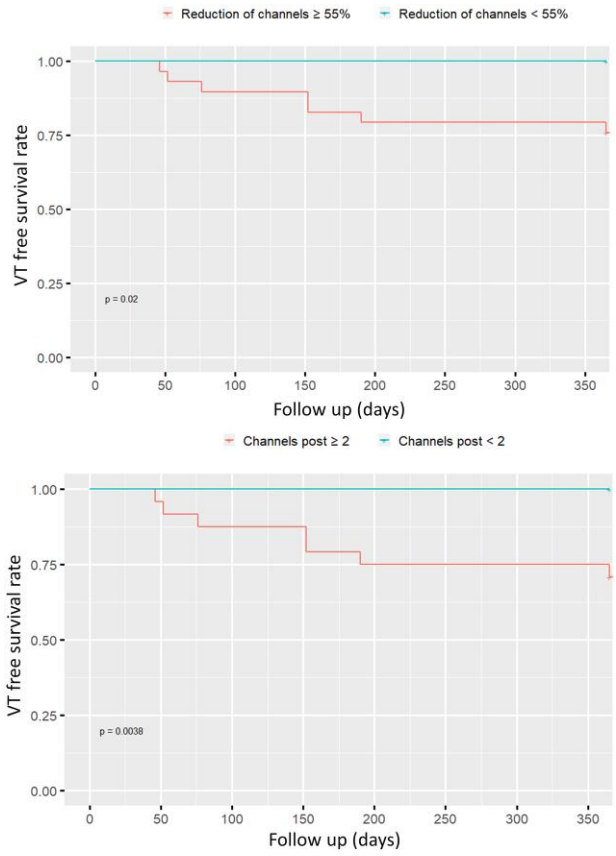

Figure 5 Kaplan–Meier VT free survival curve according to reduction of conducting channels in post-ablation CMR and the number of post-ablation LGE-CMR channels.

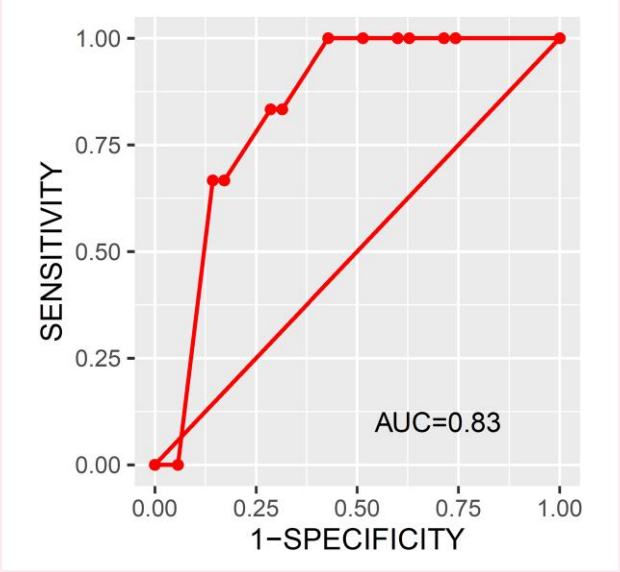

Figure 6 Receiver operating characteristic (ROC) curve of the degree of conducting channels reduction in relation to ventricular tachycardia recurrence.

the area of ablation. However, there are data in animal models[15] suggesting that visualization of 'DC' depends not only on the elapsed time between the ablation procedure and the LGE-CMR acquisition but also on the delay from contrast LGE injection to image acquisition. As the mechanism of DC is MVO, more time is required for the contrast to fill in these areas. In the mentioned study with a canine model,[15] the DC can be seen within the first 2–8 weeks after ablation, but as stated previously, the prolongation of the time to image acquisition allows the contrast to diffuse in the DC areas, resulting in a fully bright appearance of the usual scar area. At a longer follow-up (8 weeks), there was no DC detection, and the ablation lesion was typically fully bright even if image acquisition was performed 45 min after gadolinium injection, suggesting that MVO resolved in the scar core with time. In a clinical retrospective study, the typical DC appearance was not observed in cases where LGE-CMR was performed more than one month after ablation.[27] Therefore, the course of the DC and its relation to ablation lesions is still controversial. In this sense, although animal models have been used to study the time course of ablation lesions from MVO and oedema in the acute phase until its transformation to core scarring at later stages, this phenomenon is not consistent in clinical practice. Many factors can influence its occurrence, such as the presence of underlying scar tissue or local vascularization.

In our study, a DC was observed in <75% of patients, and its presence was not related to the delay between ablation and LGE-CMR (considering that all LGE-CMRs were performed between 3 and 6 months after ablation). Therefore, our study confirms that using the conventional delay of

Table 4 Association of post-ablation LGE-CMR parameters and VT recurrences

Variable	Non-recurrence	Recurrence	OR (95% CI)	*P*-value
Channels pre	2.7 ± 1.8	3.1 ± 1.7	1.13 (0.74–1.72)	0.57
Channels post	1.3 ± 1.2	3 ± 1.5	2.37 (1.19–4.72)	0.01
BZ pre (g)	24 ± 15	34 ± 14	1.04 (0.99–1.08)	0.13
BZ post (g)	22 ± 13	31 ± 24	1.03 (0.99–1.08)	0.17
Core pre (g)	12 ± 8	16 ± 10	1.05 (0.97–1.15)	0.23
Core post (g)	18 ± 10	20 ± 20	1.02 (0.95–1.08)	0.64
Channel pre (g)	8 ± 7	9 ± 4	1.00 (0.91–1.10)	0.98
Channel post (g)	3 ± 5	4 ± 4	1.03 (0.89–1.18)	0.73
% channels reduction	−49.0 ± 8.2	5 ± 3	1.02 (1.00–1.03)	0.02
% mass channels reduction	−49 ± 8.0	34 ± 7.6	1.00 (0.99–1.01)	0.65
% BZ (g) reduction	5 ± 6.6	5 ± 1.1	1.00 (0.99–1.01)	0.98
% core (g) reduction	95 ± 12.2	38 ± 1.01	1.00 (0.98–1.01)	0.26
Ischaemic (%)	81.25	100	0.56 (0.01–5.92)	0.56
Chronic kidney disease (%)	25.70	50.00	2.89 (0.49–16.97)	0.24

LGE-CMR, late gadolinium enhancement cardiac magnetic resonance; VT, ventricular tachycardia; BZ, border zone; g, grams; OR, odds ratio.

10–15 min,[14,17,22] a DC is not constant if LGE-CMR is performed out of the acute phase after ablation. More importantly, the formation of DC was not related to the acute success rate, the radiofrequency time, or the reduction in CCs (because a reduction in CCs was also observed in patients without a DC). In our opinion, this is a very important finding. There are controversial data about dark core but, considering our results, the absence of a DC does not reflect the absence of catheter-induced lesions; therefore, the changes in all scar characteristics on top of the DC must be considered to evaluate the ablation result.

Overall, our findings confirm the usefulness of LGE-CMR as a tool for evaluating VT ablation completeness. These findings, if confirmed by other studies, suggest that LGE-CMR can be useful for stratifying the risk of recurrence after ablation. Conversely, the post-ablation treatment strategy can be tailored based on the results of the ablation as assessed by LGE-CMR. In addition, post-ablation LGE-CMR is a helpful tool in cases of VT recurrence for tailoring the redo procedure based on the results of the first ablation evaluated non-invasively by LGE-CMR.

Conclusion

Post-VT ablation LGE-CMR substrate characterization can be used to evaluate ablation results in terms of CC reduction and scar homogenization. The degree of CC reduction is strongly related to VT recurrence rate. The dark core as a marker of ablation lesion is not homogeneous 3–6 months after VT ablation and is not mandatory as a marker of the ablation lesion in patients with structural heart disease.

Limitations

The main limitation of the study is that, due to the low recurrence rate, there were not enough redo procedures to ensure that scarring and CCs in the post-ablation LGE-CMR corresponded to those in the EAMs. However, the concordance of LGE-CMR with EAMs, as stated previously in the manuscript, has been proven in previous studies by our group.[14]

Regarding the LGE-CMR, a possible limitation must be addressed. The post-ablation LGE-CMR is always performed with a 1.5 Tesla scan because patients had ICD implantation, and pre-ablation LGE-CMR can be 3 Tesla in patients in whom LGE-CMR was performed before ICD implantation. It is well known that voxel size is larger in 1.5 Tesla scan, so small CCs could be underdetected. However, in most of the patients (87.5%) of patients, both pre- and post-ablation LGE-CMR was the same scan (1.5 Tesla). In addition, we have previously demonstrated that 1.5 Tesla LGE-CMR with a wideband sequence has enough accuracy to detect CCs.[14] In the same line, spatial resolution of CMR (in special 1.5 Teslas) is limited so test–retest reliability is limited. This is a common limitation of CMR technique that applies also to this study. Furthermore, within our study, four out of six patients were excluded due to artefacts or low-quality images. This decision was taken relying on the operator's criteria that presents an additional limitation.

Another limitation must be commented regarding population heterogenicity. In our study, only 6 out of 49 patients had NICM so the results must be confirmed with larger population of NICM patients. Regarding characteristics of population, only one female is included in our patients. Despite the proportion of females is always low in all VT ablation studies, is even smaller in our study so our results must be interpreted with limitations in females.

Finally, this was a single-centre study, and therefore, these results need to be confirmed in a multicentre series.

Acknowledgements

The authors want to thank Dr Peng Hu (UCLA, Los Angeles, CA) for his pioneering work on wideband LGE. We also want to thank Xiaoming Bi, PhD, and Siemens Healthineers for their support with the wideband sequence work in progress collaboration.

Conflict of interest: L.M. and J.B. report activities as a consultant, lecturer, and advisory board member for Abbott Medical, Boston Scientific, Biosense Webster, Medtronic, and Biotronik. They are also shareholders of Adas3D Medical S.L. I.R.-L. and A.P.-S. have served as a consultant for Biosense Webster, Medtronic, Boston Scientific, and Abbott Medical. M.S. reports activities as a consultant, lecturer, advisory board member, and grant recipient for Abbott Medical, Edwards Lifesciences, Sanofi, General Electric, and Medtronic. All other authors report that they have no relationships relevant to the contents of this paper to disclose.

Funding

This study was supported by Emile Letang Grand of Hospital Clinic de Barcelona/Instituto de Salud Carlos III (ISCIII) PI20/00693/CB16/11/00354, co-funded by the European Union/CIBERCV16 - CB16/11/00354 of Instituto de Salud Carlos III, Madrid and CERCA Programme/Generalitat de Catalunya. Project funded by Asociación del Ritmo SEC: SECARIT-FOR-NAC 22/008.

Data availability

No new data were generated or analysed in support of this research.

References

1. Berruezo A, Fernández-Armenta J, Andreu D, Penela D, Herczku C, Evertz R *et al.* Scar dechanneling: new method for scar-related left ventricular tachycardia substrate ablation. *Circ Arrhythm Electrophysiol* 2015;**8**:326–36.
2. Mountantonakis SE, Park RE, Frankel DS, Hutchinson MD, Dixit S, Cooper J *et al.* Relationship between voltage map "channels" and the location of critical isthmus sites in patients with post-infarction cardiomyopathy and ventricular tachycardia. *J Am Coll Cardiol* 2013;**61**:2088–95.
3. Andreu D, Ortiz-Perez JT, Boussy T, Fernandez-Armenta J, De Caralt TM, Perea RJ *et al.* Usefulness of contrast-enhanced cardiac magnetic resonance in identifying the ventricular arrhythmia substrate and the approach needed for ablation. *Eur Heart J* 2014;**35**:1316–26.
4. Andreu D, Ortiz-Perez JT, Fernandez-Armenta J, Guiu E, Acosta J, Prat-Gonzalez S *et al.* 3D delayed-enhanced magnetic resonance sequences improve conducting channel delineation prior to ventricular tachycardia ablation. *Europace* 2015;**17**:938–45.
5. Piers SRD, Tao Q, Silva M DR, Siebelink HM, Schalij MJ, Van Der Geest RJ *et al.* CMR-based identification of critical isthmus sites of ischemic and nonischemic ventricular tachycardia. *JACC Cardiovasc Imaging* 2014;**7**:774–84.
6. Vázquez-Calvo S, Casanovas JM, Garre P, Ferró E, Sánchez-Somonte P, Quinto L *et al.* Evolution of deceleration zones during ventricular tachycardia ablation and relation with cardiac magnetic resonance. *JACC Clin Electrophysiol* 2023;**9**:779–89.
7. Andreu D, Penela D, Acosta J, Perea RJ, Soto-iglesias D, De Caralt TM *et al.* Cardiac magnetic resonance–aided scar dechanneling: influence on acute and long-term outcomes. *Heart Rhythm* 2017;**14**:1121–8.
8. Roca-Luque I, Rivas-Gandara N, Francisco-Pascual J, Rodriguez-Sanchez J, Cuellar-Calabria H, Rodriguez-Palomares J *et al.* Preprocedural imaging to guide transcoronary ethanol ablation for refractory septal ventricular tachycardia. *J Cardiovasc Electrophysiol* 2019;**30**:448–56.
9. Quinto L, Sanchez-Somonte P, Alarcón F, Garre P, Castillo À, San Antonio R *et al.* Ventricular tachycardia burden reduction after substrate ablation: predictors of recurrence. *Heart Rhythm* 2021;**18**:896–904.
10. Kalin R, Stanton MS. Current clinical issues for MRI scanning of pacemaker and defibrillator patients. *Pacing Clin Electrophysiol* 2005;**28**:326–8.
11. Bhuva AN, Kellman P, Graham A, Ramlall M, Boubertakh R, Feuchter P *et al.* Clinical impact of cardiovascular magnetic resonance with optimized myocardial scar detection in patients with cardiac implantable devices. *Int J Cardiol* 2019;**279**:72–8.
12. Do DH, Eyvazian V, Bayoneta AJ, Hu P, Finn JP, Brad JS *et al.* Cardiac magnetic resonance imaging using wideband sequences in patients with nonconditional cardiac implanted electronic devices. *Heart Rhythm* 2018;**15**:218–25.
13. Hilbert S, Weber A, Nehrke K, Bornert P, Schnackenburg B, Oebel S *et al.* Artefact-free late gadolinium enhancement imaging in patients with implanted cardiac devices using a modified broadband sequence: current strategies and results from a real-world patient cohort. *Europace* 2018;**20**:801–7.
14. Roca-Luque I, Van Breukelen A, Alarcon F, Garre P, Tolosana JM, Borras R *et al.* Ventricular scar channel entrances identified by new wideband cardiac magnetic resonance sequence to guide ventricular tachycardia ablation in patients with cardiac defibrillators. *Europace* 2020;**22**:598–606.
15. Ghafoori E, Kholmovski E, Thomas S, Silvernagel J, Nathan A, Nan H *et al.* Characterization of gadolinium contrast enhancement of radiofrequency ablation lesions in predicting edema and chronic lesion size. *Circ Arrhythm Electrophysiol* 2017;**10**:1–9.
16. Celik H, Ramanan V, Barry J, Ghate S, Leber V, Oduneye S *et al.* Intrinsic contrast for characterization of acute radiofrequency ablation lesions. *Circ Arrhythm Electrophysiol* 2014;**7**:718–27.
17. Dabbagh GS, Ghannam M, Siontis KC, Attili A, Cochet H, Jais P *et al.* Magnetic resonance mapping of cathter ablation lesions after post-infarction ventricular tachycardia ablation. *JACC Cardiovasc Imaging* 2021;**14**:588–98.
18. Cronin EM, Bogun FM, Maury P, Peichl P, Vice-chair E, Chen M *et al.* 2019 HRS/EHRA/APHRS/LAHRS expert consensus statement on catheter ablation of ventricular arrhythmias. *EP Europace* 2019;**21**:1143–4.
19. Aziz Z, Shatz D, Raiman M, Upadhyay GA, Beaser AD, Besser SA *et al.* Targeted ablation of ventricular tachycardia guided by wavefront discontinuities during sinus rhythm: a new functional substrate mapping strategy. *Circulation* 2019;**140**:1383–97.
20. De Chillou C, Groben L, Magnin-poull I, Abdelaal A, Ammar S, Sellal J *et al.* Localizing the critical isthmus of postinfarct ventricular tachycardia : the value of pace-mapping during sinus rhythm. *Heart Rhythm* 2014;**11**:175–81.
21. Fernández-Armenta J, Berruezo A, Andreu D, Camara O, Silva E, Serra L *et al.* Three-dimensional architecture of scar and conducting channels based on high resolution ce-CMR insights for ventricular tachycardia ablation. *Circ Arrhythm Electrophysiol* 2013;**6**:528–37.
22. Sánchez-Somonte P, Quinto L, Garre P, Zaraket F, Alarcón F, Borràs R *et al.* Scar channels in cardiac magnetic resonance to predict appropriate therapies in primary prevention. *Heart Rhythm* 2021;**18**:1336–43.
23. van der Bijl P, Delgado V, Bax JJ. Sudden cardiac death: the role of imaging. *Int J Cardiol* 2017;**237**:15–8.
24. Linhart M, Alarcon F, Borràs R, Benito EM, Chipa F, Cozzari J *et al.* Delayed gadolinium enhancement magnetic resonance imaging detected anatomic gap length in wide circumferential pulmonary vein ablation lesions is associated with recurrence of atrial fibrillation. *Circ Arrhythm Electrophysiol* 2018;**11:e006659**:1–9.
25. Dinov B, Oebel S, Hilbert S, Loebe S, Arya A. Characteristics of the ablation lesions in cardiac magnetic resonance imaging after radiofrequency ablation of ventricular arrhythmias in relation to the procedural success. *Am Heart J* 2018;**204**:68–75.
26. Dickfield T, Kato R, Zviman MM, Lai S, Meininger G, Lardo AC *et al.* Characterization of radiofrequency ablation lesions with gadolinium-enhanced cardiovascular magnetic resonance imaging. *J Am Coll Cardiol* 2006;**47**:370–8.
27. Vunnam R, Ghzally Y, Mbbs JBM, See V, Maheshwari V, Imanli H *et al.* Ventricular arrhythmia ablation lesions detectability. *Pacing Clin Electrophysiol* 2020;**43**:314–21.